Thermosetting Bismaleimide/Reactive Rubber Blends: Curing Kinetics and Mechanical Behavior

M. ABBATE, E. MARTUSCELLI, P. MUSTO, G. RAGOSTA

National Research Council of Italy, Institute of Research and Technology of Plastic Materials, 80072 Arco Felice (Na), Italy

Received 6 May 1996; accepted 17 December 1997

ABSTRACT: A maleimido-terminated butadiene–acrylonitrile copolymer was employed as an impact modifier for a commercial thermosetting bismaleimide resin. FTIR spectroscopy was used to monitor in real time the kinetics of the curing process in this blend system at different temperatures. The toughening agent was found to produce strong effects on the kinetics and mechanism of the curing process. The fracture toughness parameters K_c and G_c showed a substantial enhancement as the rubber content in the blend was increased. Only a modest reduction of the elastic modulus and of the compressive yield stress was brought about by incorporation of the impact modifier.
 J Appl Polym Sci **65:** 979–990, 1997

INTRODUCTION

Polyimides are aromatic-heterocyclic polymeric resins which cure via crosslinking reactions or linear chain-extension reactions to give high-temperature-resistant materials.[1–4] These resins are able to maintain their excellent properties at temperatures far exceeding those of highly crosslinked epoxies. In fact, while the maximum use temperature of epoxies is about 200°C, polyimides can be used at temperatures up to 370°C. Such an outstanding temperature stability is due to the aromatic-heterocyclic structure of the polymer backbone:

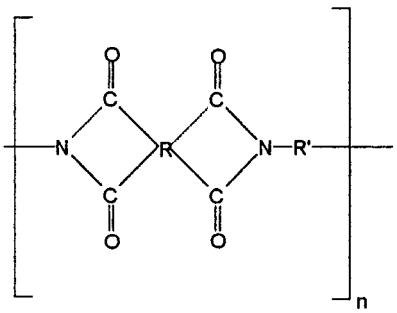

Correspondence to: P. Musto.
 CCC 0021-8995/97/050979-12

where R and R′ can be varied. This molecular structure, besides its very high thermal and thermooxidative stability, also provides high glass transition temperatures.

However, polyimides, like all the thermosetting materials, suffer a major drawback, namely, their brittleness, which is attributed to the aromatic nature and to the high crosslink density of the network. This problem is particularly relevant for the bismaleimide resins, which exhibit the highest crosslink density. Several approaches have been divised to overcome this limitation, among which the most promising are addition of reactive elastomers,[5] Michael addition chain reaction,[6,7] copolymerization with allyl-terminated copolymers, and modification with thermoplastics.[8] In a previous article,[9] interesting results in terms of toughness were achieved when a thermoplastic polyetherimide (PEI) was used as a toughening agent for a bismaleimide resin (BMI). The toughness was found to increase regularly by increasing the amount of PEI in the blend.

In the present contribution, we report on the modification of a commercial bismaleimide resin by addition of a reactive liquid rubber. In particular, an amino-terminated butadiene–acrylonitrile copolymer was chemically modified into a malei-

mido-terminated rubber and used as a toughening agent. A kinetic analysis as a function of temperature was performed on a typical blend composition and its behavior was compared with that of the neat resin in order to investigate the effect of the rubber modifier on the curing process and to identify possible chemical interactions among the blend components. The technique used to monitor in real time the conversion profiles of the various reactive species was Fourier transform infrared spectroscopy (FTIR).

The mechanical and the fracture properties of the cured materials were studied at a low and high rate of deformation. The fracture data were analyzed using the linear elastic fracture mechanics approach[10] in order to evaluate the intrinsic toughness.

EXPERIMENTAL

Materials

The bismaleimide resin commercially available as Kerimid FE 70026 (Rhone-Poulenc) was a mixture of 4,4′-bismaleimido–diphenylmethane (BMI) and tolylene–BMI in the weight ratio of 60/40:

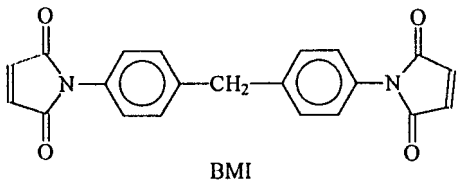

BMI

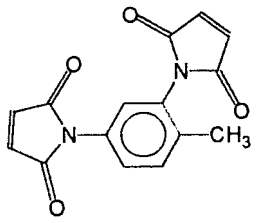

Tolylene-BMI

The resin is partially oligomerized by a diamine to improve its processability. In fact, it is a glassy solid at ambient temperature and becomes fluid at about 50°C; no free primary amino groups are present in the formulation and the curing process can be considered purely thermal. The exact molecular structure of this product is proprietary and this limits to some extent its spectroscopic characterization. Nevertheless, Kerimid 70026 was used in place of other, better-characterized BMI monomers, owing to the solubility of the reactive liquid rubber in such a matrix.

The rubber-toughening agent was a maleimido-terminated butadiene–acrylonitrile copolymer (ITBN) obtained by chemically modifying a commercially available ammino-terminated rubber (ATBN, Goodrich) having an $\bar{M}_n$ = 3600 and an acrylonitrile content of 18% wt/wt.

The reaction scheme for the preparation of the maleimido-terminated copolymer (ITBN) is the following:

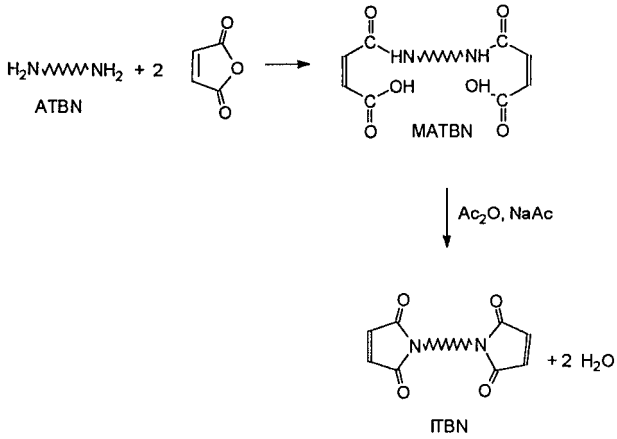

The reaction is carried out in chloroform as the solvent and proceeds in two steps: first, maleamic acid is formed by reacting the $-NH_2$ end groups with a stoichiometric amount of maleic anhydride at room temperature. Then, this intermediate (MATBN) is cyclized by adding to the solution acetic anhydride and sodium acetate. The procedure used for the preparation of the ITBN rubber as well as its spectroscopic characterization is reported elsewhere.[11]

Preparation of Kerimid/ITBN Blends

A series of blends was prepared by dissolving the ITBN rubber into the resin at 120°C for 30 min and degassing under a vacuum for additional 30 min. At the end of this step, a clear, visually homogeneous mixture was obtained. This mixture was then poured in a glass mold and cured at 180°C for 5 h and postcured at 220°C for 2 h. The codes and compositions of the investigated blends are reported in Table I.

Techniques

FTIR spectra were obtained at a 2 cm^{-1} resolution with a Perkin-Elmer System 2000 spectrometer

Table I Codes and Compositions of the Investigated Blends

Code	BMI (Wt %)	ITBN (Wt %)
B0	100	—
B4	96	4
B8	92	8
B10	90	10
B15	85	15

equipped with a deuterated triglycine sulfate detector (DTGS) and a germanium/KBr beam splitter. The recorded wavenumber range was 4000–400 cm^{-1} and 30 spectra were signal-averaged in the conventional manner to reduce the noise. The measurements were carried out on thin (1–5 μm) films cast on KBr disks from CH_2Cl_2. In all cases, the film thickness was chosen so as to keep the absorbance of the region of interest in a range where the Beer–Lambert law is obeyed. The isothermal kinetic measurements were performed in a Specac 80100 temperature chamber directly mounted in the spectrometer. This unit was driven by an Eurotherm 071 temperature controller to an accuracy of ±1°C.

Uniaxial compressive tests were made on parallelepipedal samples 12 mm long, 6.0 mm wide, and 4.0 mm thick using an Instron mechanical tester at ambient temperature and at a crosshead speed of 1 mm/min. Flexural elastic modulus measurements were performed using the same apparatus and the same testing conditions as above. The following equation was employed:

$$E = \frac{L^3 P}{4dWB^3} \quad (1)$$

where d is the displacement; P, the load at the displacement d; L, the span; and W and B, the width and the thickness of the specimen, respectively.

Three-point bending specimens were used to perform fracture tests at room temperature and at low and high strain rates. The low strain rate measurements were carried out on an Instron apparatus at a crosshead speed of 1 mm/min. The high strain rate tests were performed on a Charpy instrumented pendulum at an impact speed of 1 m/s.

For both tests, samples (60 × 6.0 × 4.0 mm) were cut from sheets of the cured materials and then sharply notched. The fracture data were analyzed according to the concepts of linear elastic fracture mechanics.[11]

The critical stress intensity factor, K_c, was calculated by means of the equation

$$K_c = \sigma Y \sqrt{a} \quad (2)$$

where σ is the nominal stress at the onset of crack propagation; a, the initial crack length; and Y, a calibration factor depending upon the specimen geometry. For three-point bending specimens, Y was given by Brown and Srawely.[12] For the determination of the critical strain energy rate, G_c, the following equation was used:

$$G_c = \frac{U}{BW\Phi} \quad (3)$$

where U is the fracture energy; B and W, the thickness and the width of the specimen, respectively; and Φ, a calibration factor which depends on the length of the notch and the size of the sample. Values of Φ were taken from Plati and Williams.[13] Fractured surfaces were coated with a thin layer of a gold–palladium alloy and then examined by scanning electron microscopy (SEM).

RESULTS AND DISCUSSION

Kinetic Analysis of the Curing Process

In Figure 1 are reported the spectra of the neat Kerimid collected at 160°C in the frequency range 3250–2700 cm^{-1}. Two peaks characteristic of the maleimide double bonds are located at 3167 and 3100 cm^{-1}. The former has been attributed to the first overtone of the C=C stretching vibration, while the latter is due to the C—H stretching mode of the bismaleimide unsaturation.[14–16] Both peaks are found to decrease with reaction time, thus confirming the gradual disappearance of maleimidic double bonds. However, the 3167 cm^{-1} peak is too low in intensity to afford a reliable quantitative evaluation. The 3100 cm^{-1} peak has a reasonable intensity but suffers from extensive overlapping with the peak at 3037 (aromatic ν_{C-H}). The spectral data were thus analyzed using subtraction spectroscopy, whereby the spectrum at time zero is subtracted from those collected at longer times:

$$A_s = A_t - \mathrm{SF} \cdot A_0$$

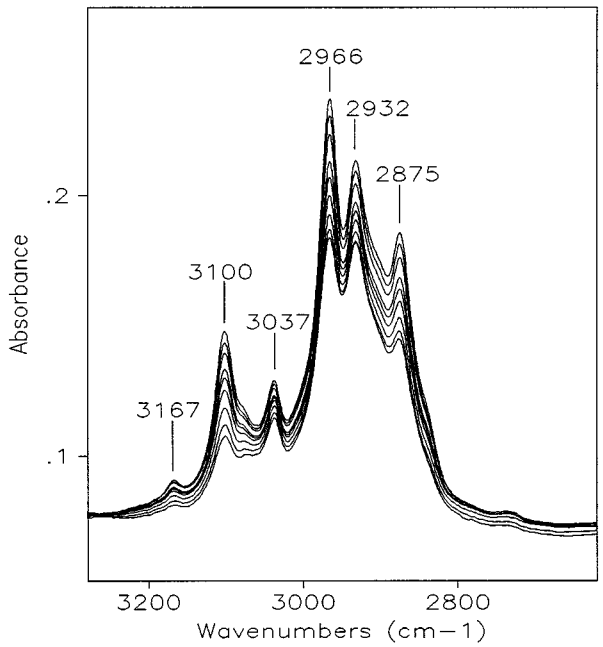

Figure 1 Real-time spectroscopic monitoring of the curing reaction of the neat Kerimid resin in the frequency range 3300–2600 cm^{-1}. Spectra were collected at 160°C.

where the subscripts s, t, and 0 denote the absorbance of the subtraction spectrum, of the spectrum collected at time t, and of the spectrum collected at time zero, respectively.

The subtraction factor (SF) allows one to compensate for differences in thickness between the spectra collected at times zero and t. Its value is obtained by reducing to the base line an internal thickness peak, i.e., a peak which is invariant with the reactants' conversion (in the present case, the aromatic absorption at 1514 cm^{-1}). It has been found that the thickness variation during the process is very limited, so that the SF is always close to unity. The main advantage in using spectral subtraction in the analysis of kinetic data relies on the fact that peaks not affected during the process (the interfering absorption at 3037 cm^{-1} in the present case) are compensated for and, hence, completely removed in the subtraction spectrum. Conversely, positive absorbances from the zero base line generally reflect molecular structures that are formed during the process, while negative absorbances reflect structures that are lost.

The subtraction spectra reported in Figure 2 in the frequency range 3200–2800 cm^{-1} clearly show the gradual development of a completely resolved negative peak of BMI at 3100 cm^{-1}, for which a linear and consistent base line can be identified. The absorbance values so evaluated can be directly used to determine the BMI conversion as a function of time.

There is a further peak, located at 827 cm^{-1}, which has been found to decrease in intensity as the curing process proceeds (see Fig. 3). Various assignments have been proposed in the literature for this absorption[15,16] and, in a recent contribution, it was tentatively ascribed to an out-of plane bending of the =C—H in the maleimide unit.[16] Its behavior during the crosslinking process seems to support strongly such an assignment; as a matter of fact, a conversion profile calculated from the intensity of this absorption is to all purposes coincident with the curve obtained by using the 3100 cm^{-1} peak and the procedure outlined above. Thus, the 827 cm^{-1} band provides a further analytical peak suitable to monitor the curing process of the bismaleimide and to cross-check the results obtained in a different frequency range.

In Figure 4 are reported the conversion, α, vs. time curves for the neat Kerimid resin at three different temperatures (160, 170, and 180°C). All the curves show an initial linear trend whose slope increases by increasing the temperature. At longer times, the reaction rates decrease substantially and the curves approach a plateau region. The final conversion increases with increasing temperature. It is noted that at 180°C the final conversion values do not exceed 50%; this is due, in part, to the rigidity of the resin, whose T_g in-

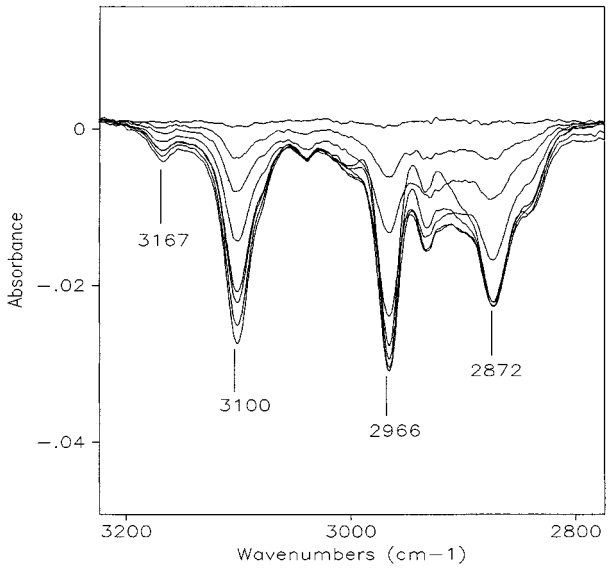

Figure 2 Spectral subtraction analysis of the data reported in Figure 1.

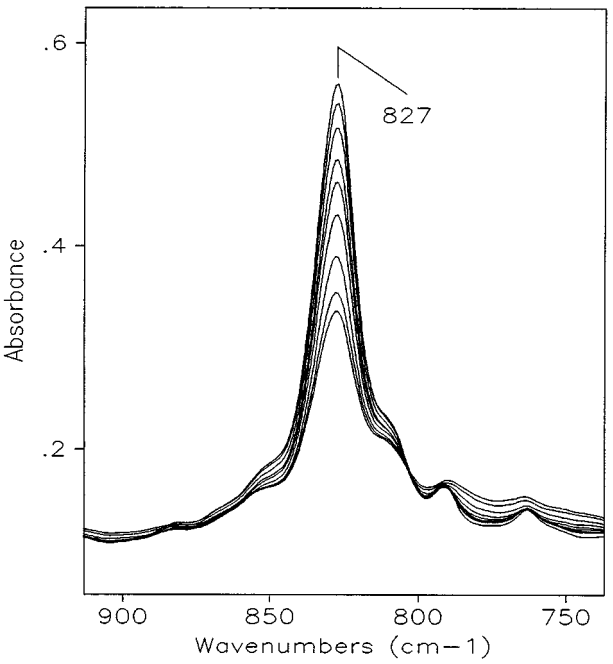

Figure 3 Real-time spectroscopic monitoring of the curing reaction of the neat Kerimid resin in the frequency range 900–750 cm^{-1}. Spectra were collected at 160°C.

creases rapidly with conversion. Thus, at α values close to 0.5, the glass transition reaches the reaction temperature and the curing process is frozen in; to achieve a more complete cure, it is necessary to process the resin at temperatures exceeding 200°C.

When the ITBN component is premixed with

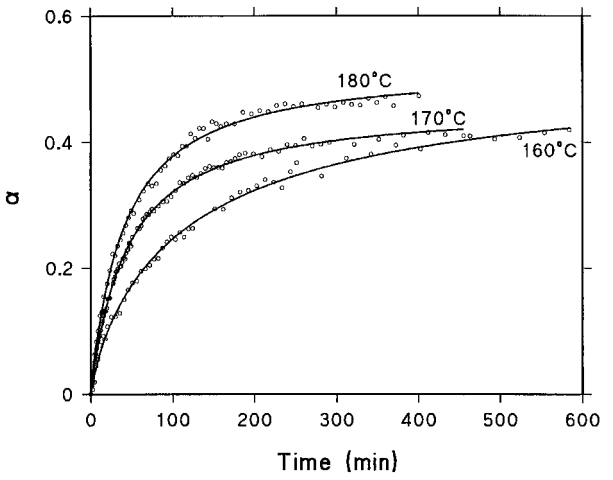

Figure 4 The conversion of bismaleimide double bonds as a function of the reaction time for the neat Kerimid resin. Temperatures as indicated.

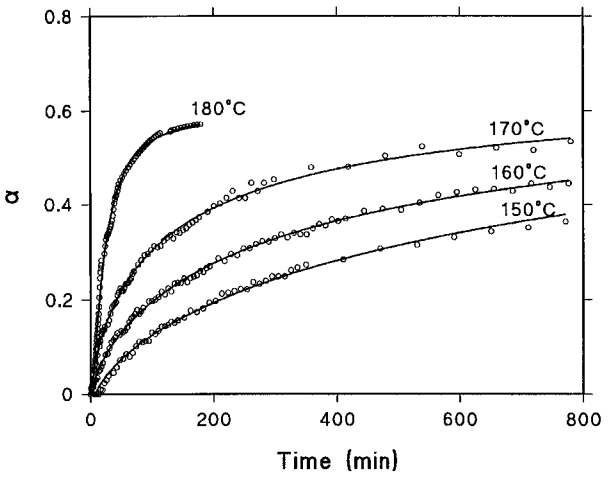

Figure 5 The conversion of bismaleimide double bonds as a function of the reaction time for the 85/15 Kerimid/ITBN blend. Reaction temperatures as indicated.

the Kerimid matrix, noticeable effects are detected in the curing kinetics. The α–t curves relative to a blend containing 15% wt/wt of ITBN at 150, 160, 170, and 180°C are reported in Figure 5.

To highlight the differences, the kinetic curves relative to neat Kerimid resin (curve A) and to the blend (curve B) at 160, 170, and 180°C are compared in Figure 6. It is readily apparent that both at 160 and 170°C the curing process in the blend is considerably retarded; in particular, the initial linear trend occurring in the neat resin is almost completely suppressed in the blend. Moreover, for the blend, owing to the slower reaction rate, a plateau region was not reached in the investigated time range although it appears that the α–t curves of the blend tend to the same final conversion values of the neat resin. However, the above retardation effect is found to depend strongly on the reaction temperature: It decreases at 170°C, while at 180°C, the situation is completely reversed. Here, both the reaction rate and the final conversion are higher in the blend than in the neat resin.

The retardation effect observed at 160 and 170°C might be accounted for by a viscosity increase occurring when the ITBN rubber is dissolved in the neat resin. This, in turn, causes a reduction in molecular mobility of the maleimide functionalities involved in the crosslinking process. As the temperature increases, such an effect is reduced because of the decreasing viscosity of the blend system and, more importantly, because of the higher rate of production of primary radi-

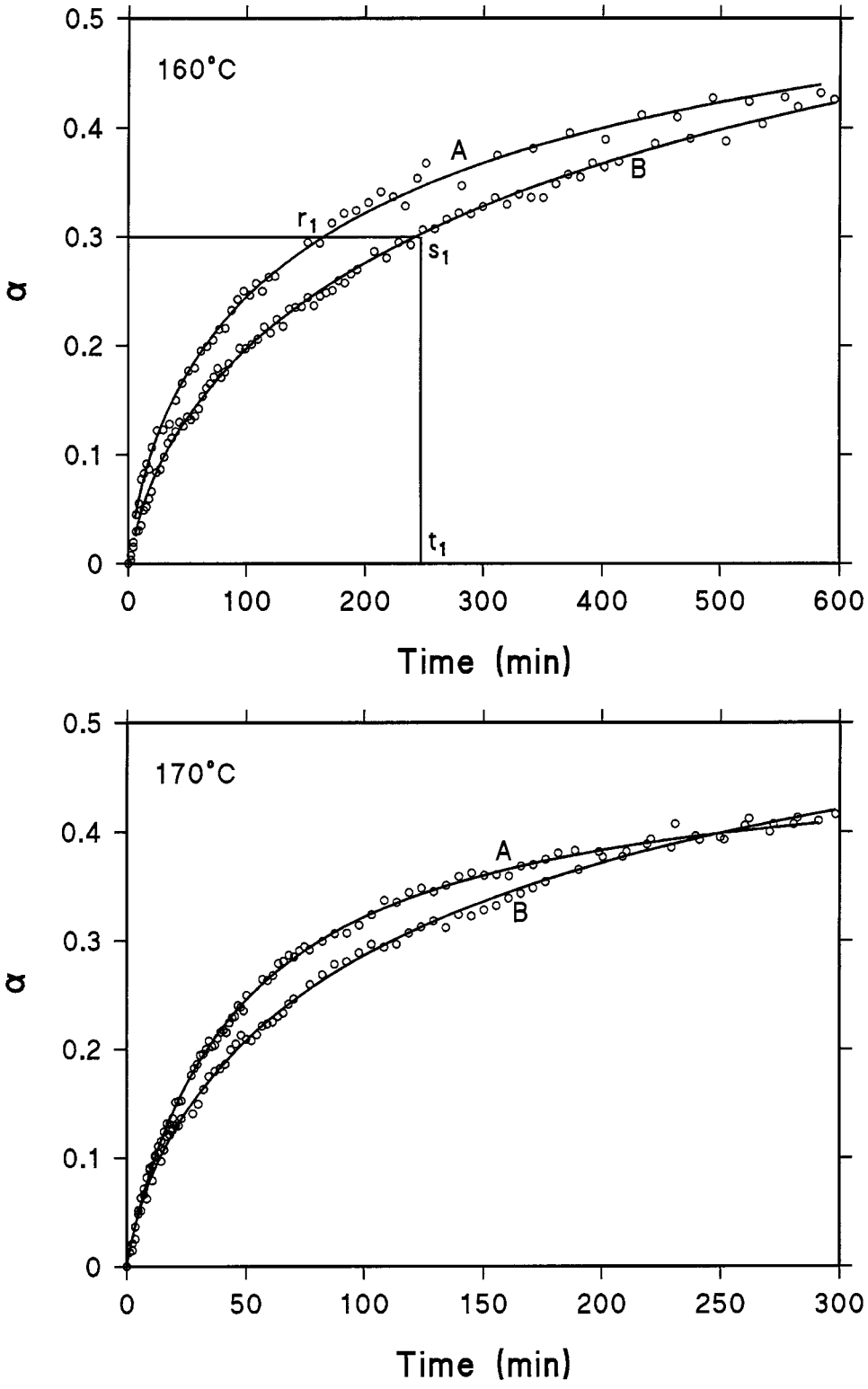

Figure 6 Comparison of the bismaleimide conversion profiles relative to the neat Kerimid resin (curve A) and to the Kerimid/ITBN 85/15 blend (curve B). Reaction temperatures as indicated.

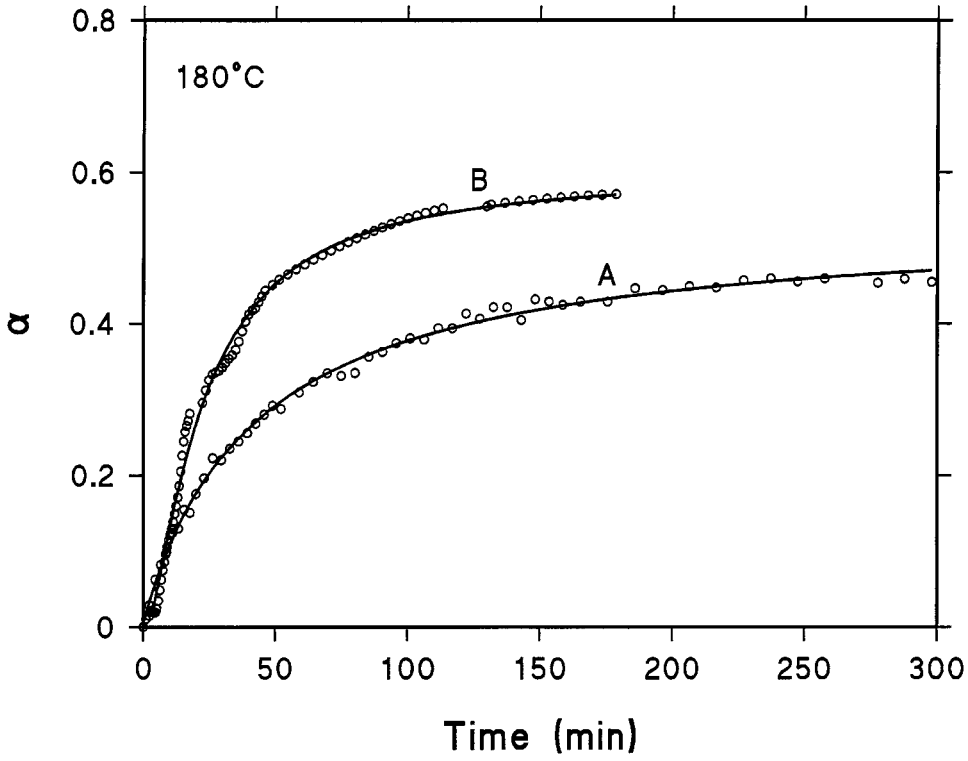

Figure 6 (*Continued from the previous page*)

calic species which renders the system less sensitive to molecular mobility effects.

The observation that at 180°C an opposite effect is found on both the reaction rate and the final conversion is not easily accounted for. One possible explanation could be the occurrence of further reaction steps which are inactive at lower temperatures. These processes involve chemical interactions between the rubber unsaturations and the bismaleimide double bonds and have the net effect of complicating the overall reaction mechanism and of accelerating the chain addition process through which the BMI network is built up. Spectroscopic evidence of the occurrence of such reactions at 180°C is discussed below.

The problem of the possible chemical interactions between the ITBN rubber and the thermosetting matrix was investigated spectroscopically. In principle, these interactions may occur either through the maleimide end groups of ITBN or by reaction of the double bonds along the ITBN backbone.

The first kind of interaction is not amenable to spectroscopic analysis since the rubber end groups yield the same signals as those of the maleimide groups of the matrix and the contribution of the two species cannot be separated. However, since alifatic bismaleimides are more reactive than are their aromatic counterparts, it is very likely that the BMI end groups of the rubber do participate in the crosslinking process through which the Kerimid network is built up.

With respect to the unsaturations present along the rubber backbone, it is well known that, in general, they may have three different configurations:

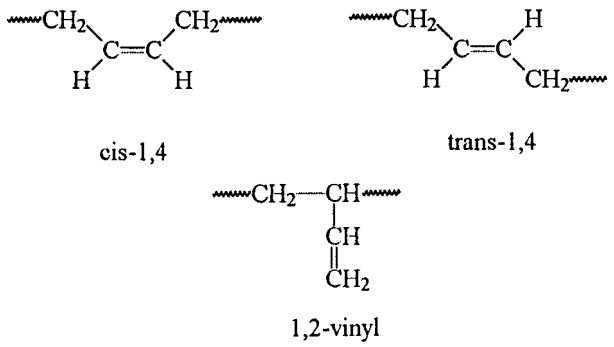

These configurations yield three distict characteristic frequencies due to the out-of-plane deformation of the =C—H bond at 730, 970, and 915 cm^{-1}, respectively.

The ITBN transmission spectrum reported in

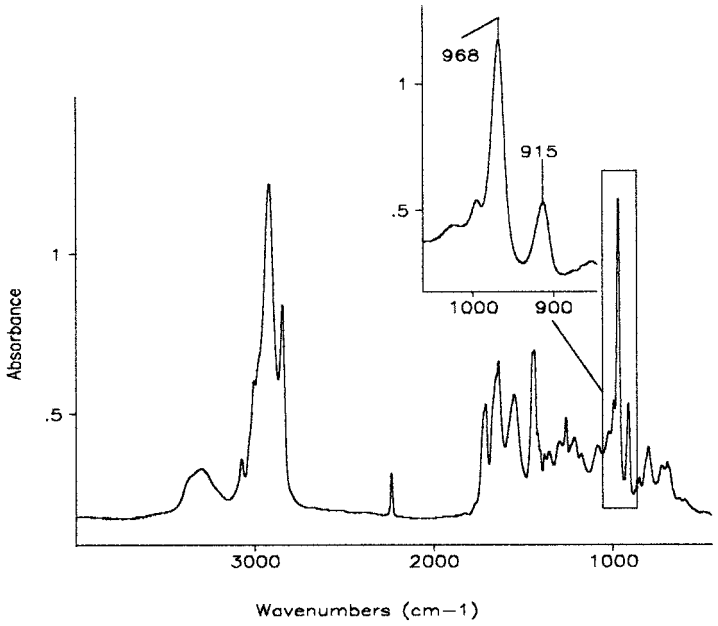

Figure 7 The ITBN transmission spectrum in the frequency range 4000–450 cm^{-1}. The inset evidences the frequency range where the characteristic group frequencies of the double bonds occur.

Figure 7 shows the presence of two well-resolved absorptions at 968 and at 915 cm^{-1}, while the characteristically broad peak at 730 cm^{-1}, distinctive of *cis*-1,4 configurations, is absent. Thus, in the ITBN copolymer, only *trans*-1,4 and 1,2-vinyl configurations are present, with the former being largely predominant. The knowledge of the ratio $\varepsilon_{trans}/\varepsilon_{1,2;v}$ (Ref. 17) allows one to evaluate quantitatively the relative population of the above configurations by using the relationship

$$\frac{C_{trans}}{C_{1,2v}} = \frac{\varepsilon_{1,2v}}{\varepsilon_{trans}} \cdot \frac{A_{trans}}{A_{1,2v}}$$

In the present case, it is found that 82.3% of monomeric units are present in the *trans*-1,4 configuration and 17.7% in the 1,2-vinyl configuration.

By using spectral subtraction spectroscopy, it has been possible to isolate the spectrum of ITBN in the region of interest from that of the blend. This was accomplished by digitally subtracting the contribution of the matrix from the blend spectrum.

A typical result of such an analysis is represented in Figure 8, where curve A refers to the initial blend spectrum taken at 160°C, while curve B is the subtraction spectrum; curve C is the ITBN spectrum at ambient temperature and is reported for comparison. It is noted that traces B and C are almost coincident, apart from a slight broadening of the peaks in the former spectrum which is due to a temperature effect. The spectral data of Figure 8 demonstrate the reliability of such an approach, but to be able to monitor the fate of the minor component in the blend, an appropriate criterion is needed to choose the reference spectrum to subtract at times other than zero. This is because both the blend and the reference spectra change quite substantially with time due to the crosslinking process and the rate of change of the two spectra are quite different.

Thus, in performing the spectral subtraction analysis, we chose to use a matrix spectrum and a blend spectrum having coincident values of conversion; the situation is schematically represented in Figure 6. To obtain the difference spectrum representative of ITBN at time t_1, the matrix spectrum corresponding to the point r_1 was subtracted from the blend spectrum corresponding to the point s_1. In this way, "clean" results were obtained over the whole time range investigated. It is noted, however, that this approach cannot be used for the kinetic curves taken at 180°C for times higher than 50 min. This is because at longer times the conversion values of the blend exceed the maximum conversion of the neat resin and a reliable reference spectrum is no longer available. In these cases, the spectral com-

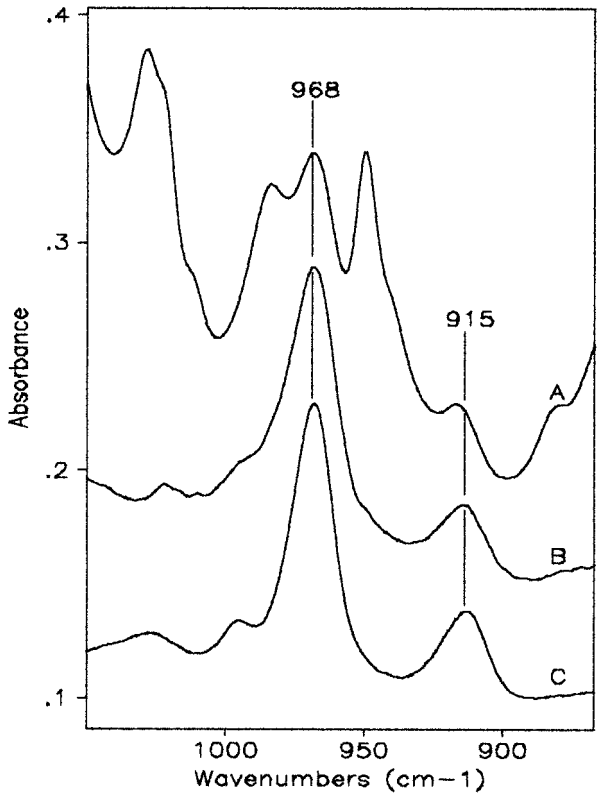

Figure 8 (A) The B15 blend spectrum in the frequency range 1050–850 cm^{-1} collected at time zero at 160°C. (B) The initial subtraction spectrum blend–neat resin at 160°C. (C) The ITBN spectrum at room temperature.

ponents at 968 and 915 cm^{-1} were separated by a curve-fitting algorithm.

In Figure 9 are reported the conversions of the *trans,* 1-4 unsaturations and those of the 1-2-vinyl unsaturations of the ITBN rubber as a function of the reaction time for the process carried out at 160 and 170°C [Fig. 9(A)] and at 180°C [Fig. 9(B)]. First, it is noted that both at 160 and at 170°C the conversion of the two unsaturated species is close to zero, which indicates that in this temperature range the double bonds along the rubber are not involved in any kind of chemical interaction.

A different picture is found at 180°C. Here, after an induction period lasting approximately 50 min, the conversion of the above species starts to increase substantially with an approximately linear trend and reaches values of about 60% by the end of the process. No evidence of a plateau region is found in the investigated time interval: The process through which the rubber unsaturations are consumed would have continued further, perhaps to completion, at longer times. Another relevant observation is that the data points relative to both the types of unsaturations can be accommodated on a single curve, which indicates a similar reactivity of both the *trans*-1,4 and the 1,2-vinyl unsaturations.

At this point, it is worth comparing the kinetic profile relative to the BMI double bonds (Fig. 5) with those of the ITBN unsaturations [Fig. 9(B)]. It is found that the rubber double bonds start to react at about 50 min when the BMI conversion is already high (45%). At this point, the BMI reaction rate has already slowed down considerably, while in the region where it was at its maximum, the ITBN unsaturations were inactive. Furthermore, in the time range where the reaction rate

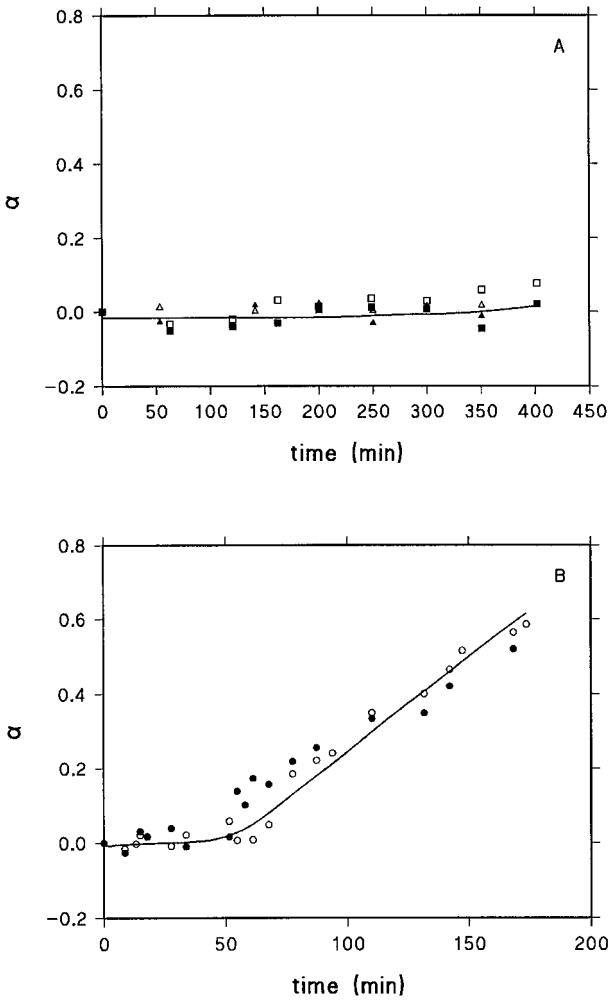

Figure 9 The conversion of the *trans,* 1-4 and of the vinyl 1-2 unsaturations of ITBN as a function of the reaction time. (□,□) 160°C; (△,△) = 170°C; (○,○) = 180°C. The open symbols refer to the 1-4-*trans* unsaturations, and the solid symbols, to the 1,2-vinyl.

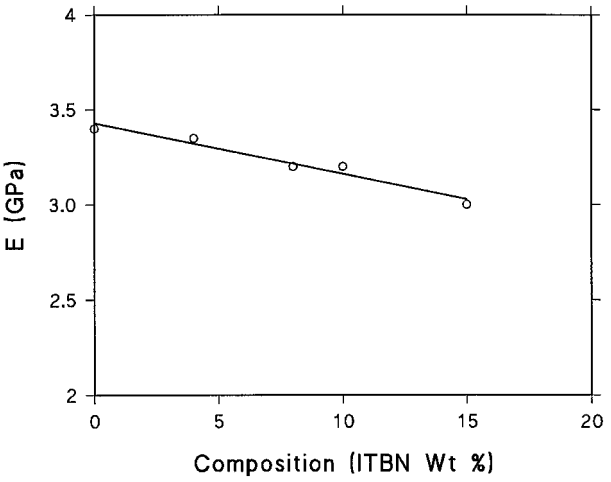

Figure 10 The flexural elastic modulus, E, for the Kerimid/ITBN blend system as a function of composition.

of the rubber double bonds is steady, the BMI reaction rate gradually reduces to zero; toward the end of the process, the BMI conversion remains constant while that of the rubber unsaturations continues to increase linearly.

In summary, it seems that the above processes are not directly correlated, as if they were following two different and independent reaction pathways. A crosslinking process of the ITBN rubber within phase-separated rubber domains initiated by catalytic amounts of BMI and/or by the maleimide end groups of the rubber would explain this effect. In this instance, the induction period would represent the time necessary to reach a critical concentration of radicalic species in the rubbery domains. This kind of mechanism has been demonstrated for polyisoprene radically crosslinked in the presence of small amounts of bismaleimide.[18,19] On the other hand, this mechanism would not account for the acceleration of the curing process of the matrix observed in the blend at 180°C and for the increase of the final BMI conversion compared to that in the neat Kerimid resin. In fact, chemical processes confined into the rubbery domains of a phase-separated system would hardly affect the overall curing mechanism of the BMI continuous phase. Furthermore, no evidence of phase separation was revealed by SEM morphological analysis.

The experimental data just discussed cannot be considered conclusive and further investigations on the molecular structure realized upon curing in such a complex network, possibly employing other spectroscopic techniques, are in order to fully account for the experimental observations. However, at temperatures of 180°C and above, extensive chemical interactions between BMI and ITBN can be anticipated which involve both the maleimide end groups and the backbone unsaturations of the rubber.

Mechanical and Fracture Properties

The Young's modulus, E, evaluated according to eq. (1), is reported in Figure 10 as a function of blend composition. As expected, the modulus decreases gradually and in a linear fashion with increasing the amount of rubber. However, only a modest reduction of E is brought about by the addition of 15% wt of ITBN. To predict large strain properties, the yielding behavior of the investigated blends was examined under a uniaxial compression mode. Typical stress–strain curves are shown in Figure 11. It can be observed that, when loaded in compression, all the samples yield and flow, contrary to what happens in tension where they exhibit a completely brittle behavior. The compressive yield stress, σ_{cy}, evaluated as indicated in Figure 11, is plotted as a function of blend composition in Figure 12. As for the modulus data, the yield stress decreases as the amount of rubber in the blend is increased. The modulus and the yield stress results indicate that the presence of the ITBN rubber makes the matrix easier to be plastically deformed under loading.

The fracture behavior of the investigated blend compositions was examined at a low rate of defor-

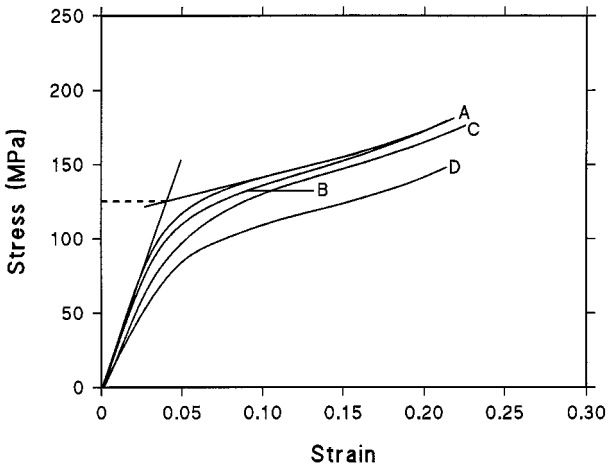

Figure 11 Compressive stress–strain curves at ambient temperature and at a crosshead speed of 1 mm/min: (A) neat resin; (B) B4 blend; (C) B10 blend; (D) B15 blend.

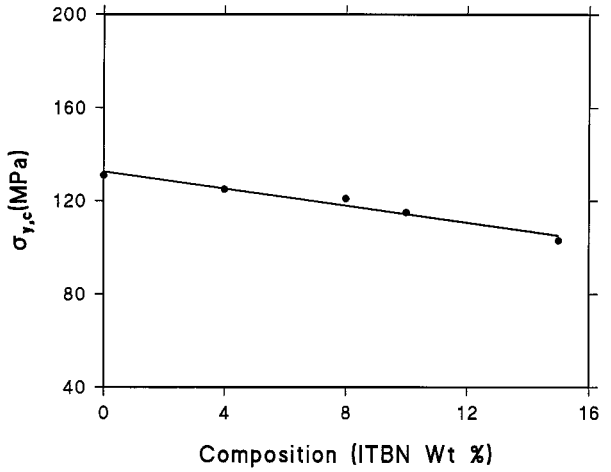

Figure 12 Compressive yield stress, $\sigma_{y,c}$, as a function of blend composition.

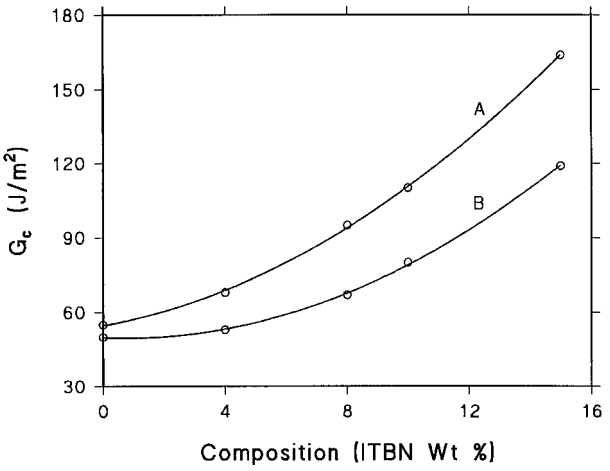

Figure 14 The critical strain energy release rate, G_c, for the Kerimid/ITBN blend system as a function of composition at high (curve B) and low (curve A) deformation rate.

mation (1 mm/min) and under impact conditions (1 m/s). The critical stress-intensity factor, K_c, using the eq. (2) is reported in Figure 13. The pure Kerimid resin exhibits low values of K_c in both test conditions, according to its poor resistance to crack propagation. For the blends, the parameter K_c increases linearly with increasing rubber content. Similar results are found when the fracture data are expressed through the parameter G_c (see Fig. 14). In this case, for the low-speed tests, an increase of about three times is achieved with respect to the value of the net resin for the 85/15 blend composition.

The observed enhancement in toughness could be due to the incorporation, during the curing process, of flexible rubber chains within the thermosetting network which enhances its ability to be plastically deformed in the vicinity of the crack tip. This hypothesis is confirmed by the morphological analysis, performed by scanning electron microscopy, on the fracture surfaces of blends of different compositions. Such an analysis did not reveal any evidence of a dispersed second phase, even at very high magnification.

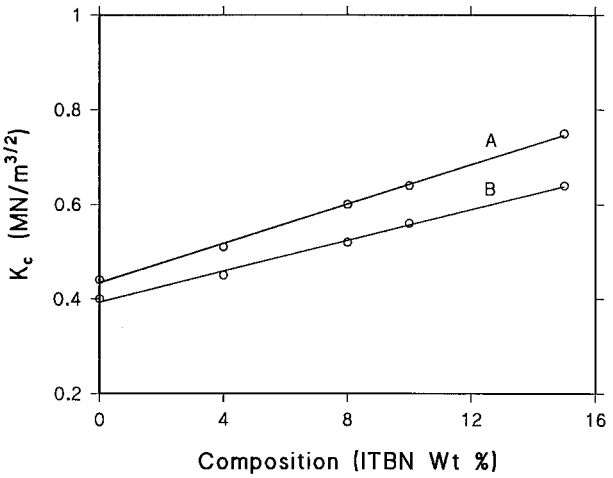

Figure 13 The critical stress intensity factor, K_c, for the Kerimid/ITBN blend system as a function of composition at high (curve B) and low (curve A) deformation rate.

Dynamic mechanical measurements were also performed to obtain further information on the phase structure of the system. For all the samples tested, no relaxation peak was observed in the temperature range of the ITBN glass transition (around −50°C). With respect to the main relaxation of the Kerimid resin, it was very difficult to detect since extensive thermal degradation took place concurrently with the onset of large-scale molecular mobility, at temperatures above 360°C. Therefore, the dynamic mechanical data, together with the morphological analysis, do suggest the occurrence of a single-phase homogeneous system after the curing and postcuring processes.

CONCLUSIONS

A maleimido-terminated butadiene–acrylonitrile copolymer was used as a toughening agent for a thermosetting bismaleimide resin (Kerimid FE 70026). The kinetics of the curing process of the blend matrix with and without the rubber mod-

ifier was investigated at different temperatures by FTIR spectroscopy. It was found that the toughening agent has a profound effect on the kinetics and mechanism of the curing process of the bismaleimide resin. In particular, below 180°C, a considerable retardation was observed, while an opposite effect was found at higher temperature. FTIR subtraction analysis demonstrated that up to 170°C the carbon–carbon double bonds along the rubber backbone do not take part in the curing process. However, at 180°C, both the 1,4-*cis* and the 1,2-vinyl unsaturations of the ITBN are found to undergo chemical reaction.

The SEM analysis showed no evidence of a phase separation of the rubber component after the curing and postcuring processes. The mechanical properties, such as the elastic modulus and the compressive yield stress, exhibited a modest reduction with increasing the amount of rubber in the blend. However, the fracture toughness parameters (K_c and G_c) evaluated at low and high rates of deformation showed a substantial enhancement as a function of the modifier's content. Such an effect was attributed to the chemical incorporation of rubber chains within the thermosetting network, which increases its ability to be plastically deformed under loading.

REFERENCES

1. V. Crivello, *J. Polym. Sci. Polym. Chem. Ed.,* **11,** 1185 (1973).
2. I. K. Varma, Sangita, and D. S. Varma, *J. Polym. Sci. Polym. Chem. Ed.,* **22,** 1419 (1984).
3. J. E. White and M. D. Scaia, *Polymer,* **25,** 850 (1984).
4. C. E. Browing, in *Advanced Thermoset Composites,* J. M. Margolis, Ed., Van Nostrand Reinhold, New York, 1986.
5. A. J. Kinlock and S. J. Shaw, *Am. Chem. Soc. Polym. Mater. Sci. Eng.,* **49,** 307 (1983).
6. M. Bergain, A. Combet, and P. Grosjean, Br. Pat. Spec. 1,190,718 (1973).
7. H. D. Stenzerberger, U.S. Pat. 4,303,779 (1981).
8. H. D. Stenzenberger, W. Romer, M. Herzog, and P. Konig, *33rd Int. SAMPE Symp.,* **33,** 1546 (1988).
9. V. Di Liello, E. Martuscelli, P. Musto, G. Ragosta, and G. Scarinzi, *Angew. Makromol. Chem.,* **223,** 93 (1993).
10. J. G. Williams, *Fracture Mechanics of Polymers,* Wiley, New York, 1984.
11. M. Abbate, E. Martuscelli, P. Musto, G. Ragosta, and M. Leonardi, to appear.
12. W. F. Brown and J. Srawley, ASTM STP4, American Society for Testing and Materials, Philadelphia, 1966, p. 13.
13. E. Plati and J. G. Williams, *Polym. Eng. Sci.,* **15,** 470 (1975).
14. D. O. Hummel, K. U. Heinen, H. Stenzenberger, and H. Siesler, *J. Appl. Polym. Sci.,* **18,** 2015 (1974).
15. C. Di Giulio, M. Gautier, and B. Jasse, *J. Appl. Polym. Sci.,* **29,** 1771 (1984).
16. S. F. Parker, S. M. Mason, and K. P. J. Williams, *Spectrochim. Acta,* **46A,** 121 (1990).
17. Silas, Yales, and Thornton, *Anal. Chem.,* **31,** 529 (1959).
18. S. Takeda and H. Kakiuchi, *J. Appl. Polym. Sci.,* **35,** 1351 (1988).
19. P. Kovacic and R. W. Hein, *J. Am. Chem. Soc.,* **81,** 1190 (1959).